

This article was downloaded by:

On: 25 January 2011

Access details: *Access Details: Free Access*

Publisher *Taylor & Francis*

Informa Ltd Registered in England and Wales Registered Number: 1072954 Registered office: Mortimer House, 37-41 Mortimer Street, London W1T 3JH, UK



## Separation Science and Technology

Publication details, including instructions for authors and subscription information:

<http://www.informaworld.com/smpp/title~content=t713708471>

### Floc Formation, Size Distribution, and its Transformation Detected by Online Laser Particle Counter

G. R. Xu<sup>a</sup>; C. S. B. Fitzpatrick<sup>b</sup>; J. Gregory<sup>b</sup>

<sup>a</sup> School of Municipal and Environmental Engineering, Harbin Institute of Technology, China <sup>b</sup> Dept. of Civil, Environmental and Geomatic Engineering, University College London, London

**To cite this Article** Xu, G. R. , Fitzpatrick, C. S. B. and Gregory, J.(2008) 'Floc Formation, Size Distribution, and its Transformation Detected by Online Laser Particle Counter', *Separation Science and Technology*, 43: 7, 1725 — 1736

**To link to this Article:** DOI: 10.1080/01496390801973706

URL: <http://dx.doi.org/10.1080/01496390801973706>

## PLEASE SCROLL DOWN FOR ARTICLE

Full terms and conditions of use: <http://www.informaworld.com/terms-and-conditions-of-access.pdf>

This article may be used for research, teaching and private study purposes. Any substantial or systematic reproduction, re-distribution, re-selling, loan or sub-licensing, systematic supply or distribution in any form to anyone is expressly forbidden.

The publisher does not give any warranty express or implied or make any representation that the contents will be complete or accurate or up to date. The accuracy of any instructions, formulae and drug doses should be independently verified with primary sources. The publisher shall not be liable for any loss, actions, claims, proceedings, demand or costs or damages whatsoever or howsoever caused arising directly or indirectly in connection with or arising out of the use of this material.

## Floc Formation, Size Distribution, and its Transformation Detected by Online Laser Particle Counter

G. R. Xu,<sup>1</sup> C. S. B. Fitzpatrick,<sup>2</sup> and J. Gregory<sup>2</sup>

<sup>1</sup>School of Municipal and Environmental Engineering, Harbin Institute of Technology, China

<sup>2</sup>Dept. of Civil, Environmental and Geomatic Engineering, University College London, London

**Abstract:** Coagulation and flocculation are widely applied in water and wastewater treatment. Removal of suspended particles is essential in water treatment and greatly depends upon the performance of the coagulant and the production of flocs with suitable properties. For monitoring floc size, formation, and size transformation, no particle size method now can be considered ideal. In this work an on-line laser particle counter was used to follow coagulation with aluminum sulfate. The experiments showed that the floc formation and floc size distribution could be well monitored. The results showed that it is feasible to use particle counting for dosage control and for monitoring changes in floc formation, transformation and size distribution.

**Keywords:** Coagulation, flocculation, particle counter, floc size

### INTRODUCTION

Coagulation has been long investigated by many means. Flocs are highly irregular and porous and so their scattering patterns are likely to be very different than for equivalent solid spheres of the same material in

Received 1 July 2007, Accepted 8 January 2008

Address correspondence to C. S. B. Fitzpatrick, Dept. of Civil, Environmental and Geomatic Engineering, University College London, Gower Street, London WC1E 6BT. E-mail: c.fitzpatrick@ucl.ac.uk

light scattering devices. For dosing control and monitoring floc size and flocculation kinetics online, no method now can be considered ideal (1).

Streaming current detector (SCD) is used mainly for coagulant dosage control (2). In this method the current between electrodes at the upper and lower ends of a cylinder is monitored and this is related to the electrokinetic charge of colloidal materials in the sample. When the streaming current is around zero, it can usually be assumed that the colloidal charge has been neutralized. A disadvantage of the SCD is that its signal is usually affected by fouling of the detector especially by organic matter.

Dynamic systems have been employed using the Photometric Dispersion Analyzer (PDA) to give an indication of floc size (3, 4). In this technique, a narrow light beam is passed through a flowing suspension. The transmitted light intensity (dc value) is measured along with the root mean square value of the fluctuating component (rms). The ratio of the rms: dc gives a very sensitive indication of particle aggregation and is known as the flocculation index.

The PDA is reported to be a very good and easy to use comparative tool showing qualitative changes in floc aggregation (5). However, the instrument is unable to give an absolute particle size for comparison with other techniques. In addition, the FI is an indicator of both particle size and particle number (6). As such there is no way of knowing the precise contribution of each of these components in the final FI value. However, the aggregate size is probably the over-riding factor as the previous work has shown that when flocs grow larger the FI value always increases.

A combination of photography/video and image analysis has also been used to monitor floc suspensions, such that a flocculated suspension can be observed by capturing images of a stirred suspension by focusing on a plane a short distance (0.3 – 1 cm) behind the wall of the vessel containing the suspension (7–10). Calibration is achieved by focusing on a graticule suspended into the tank prior to flocculation experiments. The advent of powerful digital and CCD cameras and comprehensive image analysis software has allowed much quicker measurements and so many different floc size measurements can be made from floc samples (11).

Particle size instruments that use laser scattering to determine particle size are available (12, 13). The light scattering instruments measure particle size by passing a laser beam through a suspension of particles. These techniques rely upon a constant flow of the suspension through the instrument during the measurement cycle (14). This feature has been harnessed to allow the development of a cost-effective, less destructive, and online methodology for measuring floc size (12, 13).

The objective of the present investigation is to establish a laser detection system to examine floc formation, transformation, breakage, and reformation with clay suspensions, using aluminum sulfate as a coagulant and to test the feasibility of using a Particle Counter for dosage control, and for measuring floc formation, transformation, and size distribution in coagulation and flocculation processes.

## MATERIALS AND METHODS

Kaolin clay (Imerys, St Austell, and Cornwall, UK) was used as a model suspension. The particle size distribution is rather broad, with a mean size of around 3  $\mu\text{m}$ . For the flocculation tests, it was diluted in London tap water to give a clay concentration of 10  $\text{mg L}^{-1}$ . London tap water has high total hardness (ca. 280  $\text{mg L}^{-1}$  as  $\text{CaCO}_3$ ) and alkalinity (ca. 240  $\text{mg L}^{-1}$  as  $\text{CaCO}_3$ ) and a pH of around 7.4. Aluminum sulfate hydrate ( $\text{Al}_2(\text{SO}_4)_3 \cdot 16 \text{H}_2\text{O}$ ; Fisons, >96%), ("alum") was used.

The test suspension was contained in 2 L beakers with stirrer units from a Flocculator 90, semi-automatic jar test device, with an axial impeller (Kemira Kemwater, Helsingborg, Sweden). This equipment enables the rapid mixing and slow stirring speeds and times to be pre-set. Suspension (10  $\text{mg L}^{-1}$  kaolin in London tap water) was used in this test. The standard test procedure was modified as follows: Coagulant was dosed and the suspension was stirred at 400 rpm for 20 s. Then the stirring speed was reduced to 50 rpm and held at this value for the required time (10 min), followed by a settling period of 15 min. The effective shear rates (G values) corresponding to these stirring speeds were 23  $\text{s}^{-1}$  (50 rpm) and 518  $\text{s}^{-1}$  (400 rpm) (15).

An online laser particle counter (Met One) was used. It was able to record counts in 6 separate size channels, and the ranges are 2–3  $\mu\text{m}$ , 3–5  $\mu\text{m}$ , 5–7  $\mu\text{m}$ , 7–10  $\mu\text{m}$ , 10–15  $\mu\text{m}$ , and >15  $\mu\text{m}$ , respectively. Readings were taken every 15 s and the results were stored in a computer for subsequent analysis. For dynamic monitoring, a sample from the beaker was conveyed through transparent plastic tubing (3 mm i.d.) by means of a peristaltic pump, and the plastic was fixed along the wall and the sampling site is 6 cm to the bottom. The volume needed for analysis is 100  $\text{mL min}^{-1}$ . The sample was not taken during the sedimentation, and it was resumed after sedimentation. The sample was not re-injected in the beaker after measuring the size distribution. The pump was located after the particle counter instrument to avoid the effects of possible floc breakage in the pinch portion of the pump.

## RESULTS AND DISCUSSION

Figures 1 to 3 illustrate the effects of Alum dosing in floc formation, size distribution and transformation with various dosages in coagulation, flocculation and sedimentation.

From Figure 1, it can be seen that at first, 2–3  $\mu\text{m}$  flocs reach maximum counts and then 3–5  $\mu\text{m}$ , 5–7  $\mu\text{m}$ , 7–10  $\mu\text{m}$ , the 10–15  $\mu\text{m}$  and >15  $\mu\text{m}$ , flocs reach their maximum counts respectively. This means that the smaller particles with size below 2  $\mu\text{m}$  (particle counter lower detection limit) form larger flocs to 2–3  $\mu\text{m}$  initially, and then the 2–3  $\mu\text{m}$  range particles aggregate to larger ones such as 3–5  $\mu\text{m}$ , 5–7  $\mu\text{m}$ , 7–10  $\mu\text{m}$ , the

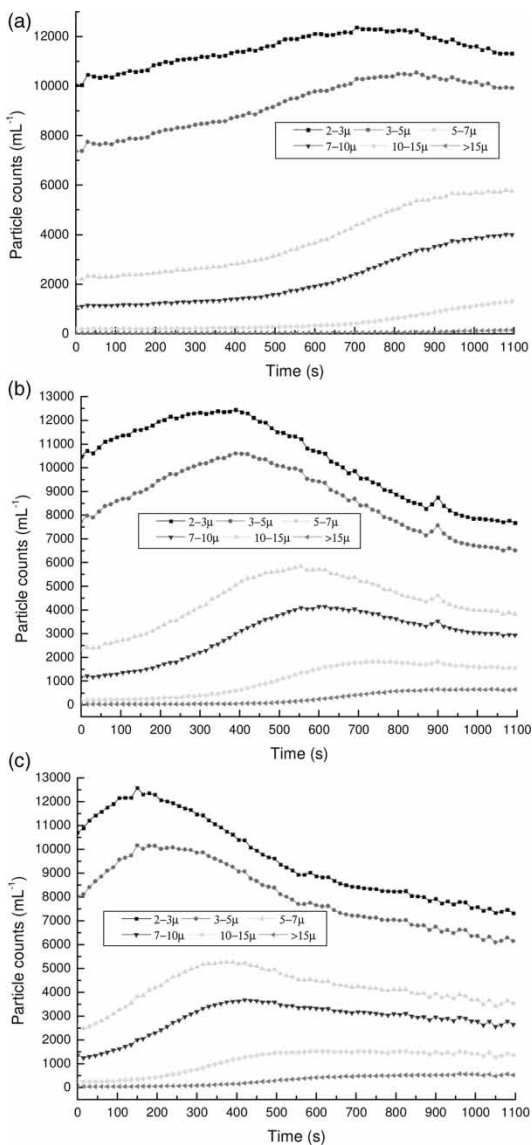


**Figure 1.** (a) Floc formation, size distribution and transformation at  $0.3 \text{ mg L}^{-1}$  (Al); (b) Floc formation, size distribution and transformation at  $0.6 \text{ mg L}^{-1}$  (Al); (c) Floc formation, size distribution and transformation at  $1.0 \text{ mg L}^{-1}$  (Al); (d) Floc formation, size distribution and transformation at  $1.6 \text{ mg L}^{-1}$  (Al); (e) Floc formation, size distribution and transformation at  $2.0 \text{ mg L}^{-1}$  (Al); (f) Floc formation, size distribution and transformation at  $2.3 \text{ mg L}^{-1}$  (Al); (g) Floc formation, size distribution and transformation at  $3.0 \text{ mg L}^{-1}$  (Al).

(continued)

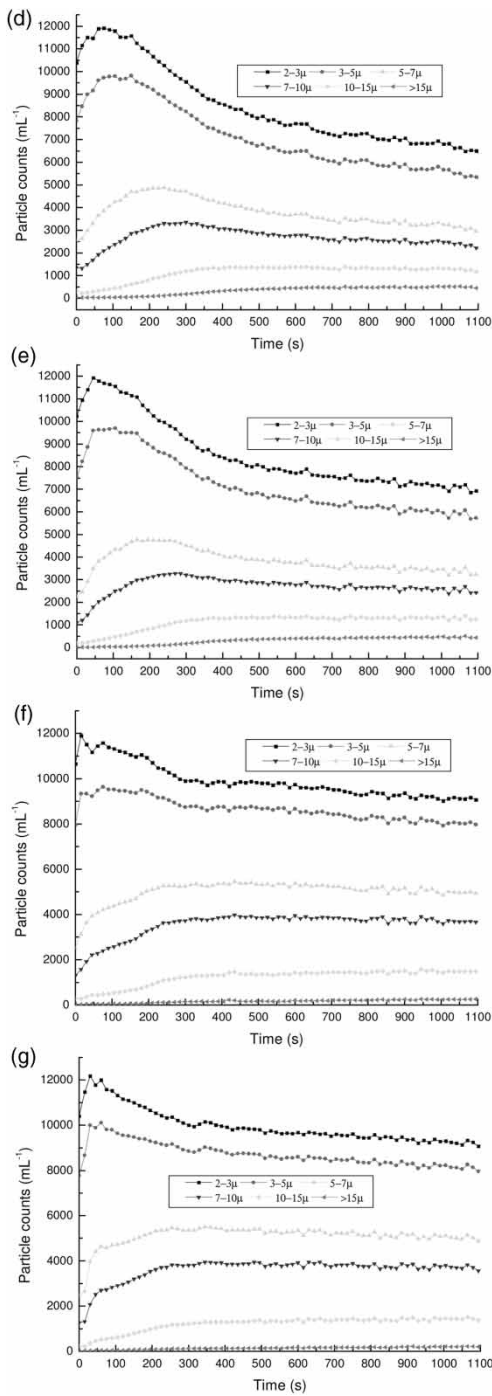
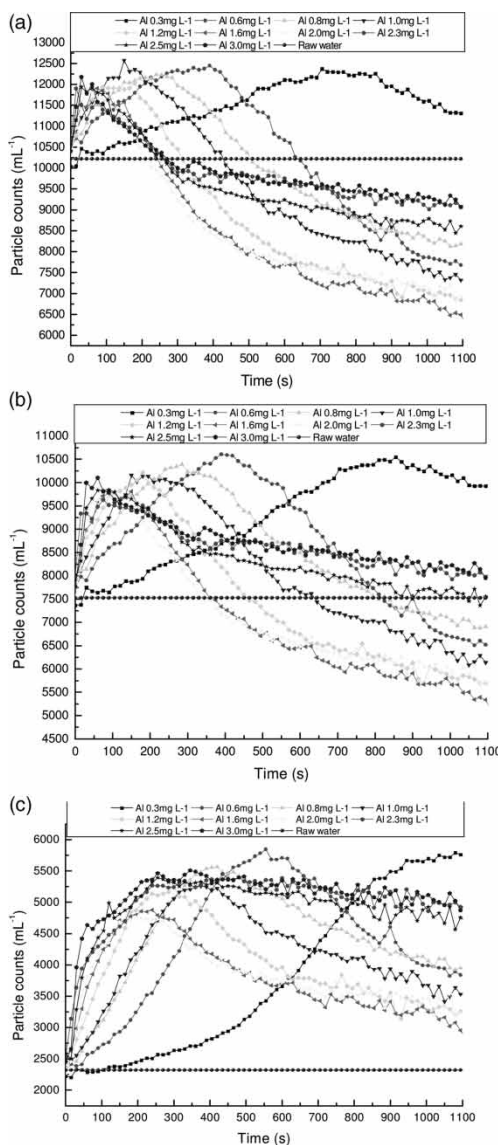


Figure 1. Continued.



**Figure 2.** (a) 2–3  $\mu\text{m}$  floc formation and transformation with various dosages coagulation; (b) 3–5  $\mu\text{m}$  floc formation and transformation with various dosages coagulation; (c) 5–7  $\mu\text{m}$  floc formation and transformation with various dosages coagulation; (d) 7–10  $\mu\text{m}$  floc formation and transformation with various dosages coagulation; (e) 10–15  $\mu\text{m}$  floc formation and transformation with various dosages coagulation; (f) >15  $\mu\text{m}$  floc formation and transformation with various dosages coagulation.

(continued)

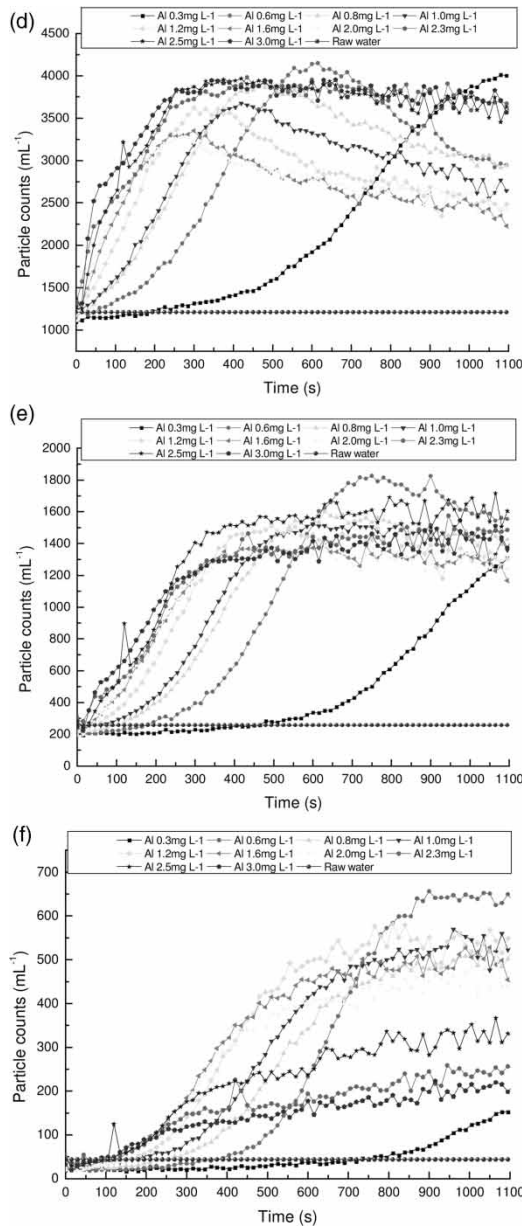
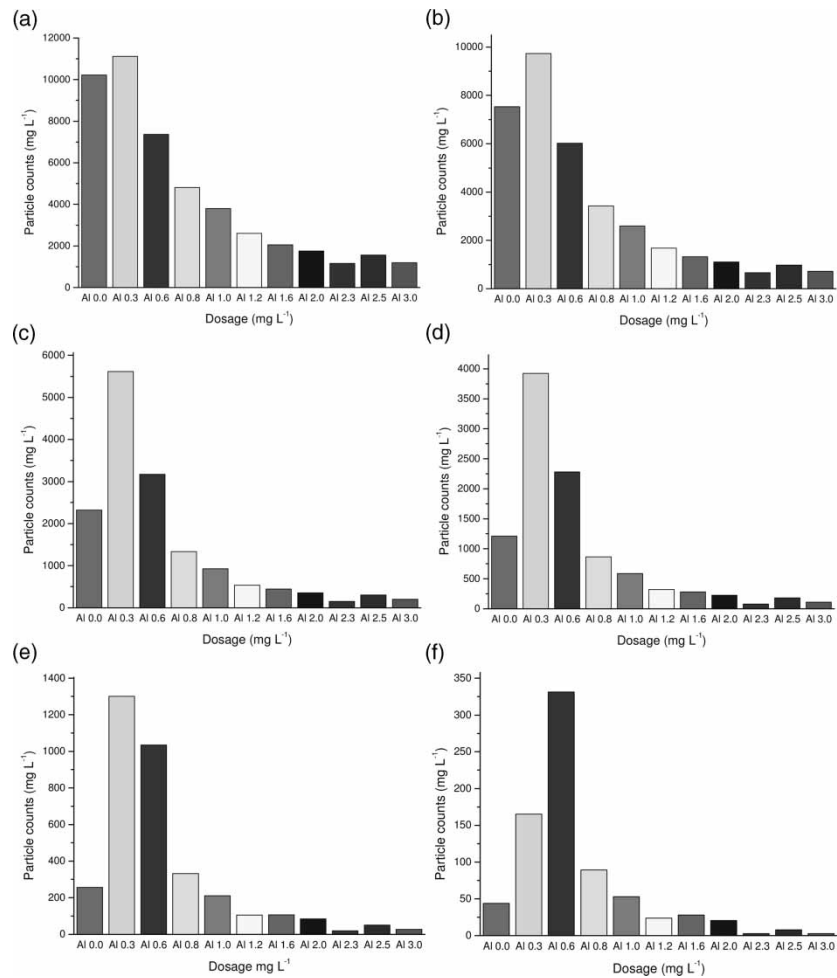


Figure 2. Continued.

10–15  $\mu\text{m}$ , and  $>15 \mu\text{m}$  progressively. So the particle or floc growth kinetics can be shown with by the floc counts very clearly.

Also the higher the coagulant dose the shorter the time to reach the maxima. The growth slope becomes sharper and sharper with the more

coagulant added. For example, in Figure 1a at the dose of 0.3 mg/L, all the particle counts rise slowly, and from Fig. 3 it can be seen that the coagulant used is not enough; From Figure 1.2–1.6, the 2–3  $\mu\text{m}$  floc attains peak counts at about 400 s (Al:0.6 mg  $\text{L}^{-1}$ ), 150 s (Al:1.0 mg  $\text{L}^{-1}$ ), 70 s (Al:1.6 mg  $\text{L}^{-1}$ ), 50 s (Al:2.0 mg  $\text{L}^{-1}$ ), 20's (Al:2.3 mg  $\text{L}^{-1}$ ) respectively, and then the amounts decrease gradually to form bigger flocs. This means that higher coagulant dosages can accelerate the coagulation stage and give shorter smaller floc growth times.



**Figure 3.** (a) 2–3  $\mu\text{m}$  particle sedimentation results with various dosages; (b) 3–5  $\mu\text{m}$  particle sedimentation results with various dosages; (c) 5–7  $\mu\text{m}$  particle sedimentation results with various dosages; (d) 7–10  $\mu\text{m}$  particle sedimentation results with various dosages; (e) 10–15  $\mu\text{m}$  particle sedimentation results with various dosages; (f)  $>15\mu\text{m}$  particle sedimentation results with various dosages.

From Fig. 2, it can be seen that 2–3  $\mu\text{m}$ , 3–5  $\mu\text{m}$ , 5–7  $\mu\text{m}$  and 7–10  $\mu\text{m}$  particles first increase rapidly (in the coagulation stage) and then decrease slowly (during the flocculation stage), but  $>15\ \mu\text{m}$  counts go up slowly throughout the flocculation stage. The growth rate has good relation to the dosage; as more coagulant is added, the peak counts occur earlier. From the decreased counts at the flocculation stage it can be seen that there is an optimum dosage range for the floc size transformation. The results show that the optimum range is from 1.0 to 2.0  $\text{mg L}^{-1}$ ; with little further change as the dosage exceeds 2.0  $\text{mg L}^{-1}$  at the flocculation stage. But from Fig. 3 it appears that the sedimentation results are not as good in the range of 1.0 to 2.0  $\text{mg L}^{-1}$ , as in the dosage range 2.0–3.0  $\text{mg L}^{-1}$ .

It is shown in Fig. 3 that there is an optimal dose range and the results correlate well with the floc growth curves shown in Fig. 1 and Fig. 2.

From Fig. 2 it can be seen that the particle counts growth curves (growth rate) can not be separated very clearly at the range of 2–3  $\mu\text{m}$ , 3–5  $\mu\text{m}$ , 5–7  $\mu\text{m}$  in the growth stage, but at the range of 7–10  $\mu\text{m}$  and 10–15  $\mu\text{m}$ , the growth rate could be distinguished very well in 0–200 s or 100–200 s. In the range of larger than 15  $\mu\text{m}$  the growth curve is in another form and different from previous data. So from these data, using an appropriate floc size range (such as 7–10  $\mu\text{m}$  or 10–15  $\mu\text{m}$ ) and opportune growth time stage (such as 0–200 s or 100–200 s), an optimum dosage signal could be generated. Also the floc size distribution and its transformation can be monitored very easily, which could be used to evaluate the influence of various factors in coagulation and flocculation.

To analyze the characteristics of the flocs counts curves with various dosages, some curves were analyzed with fitting equation in Fig. 2d and Fig. 2e. Table 1 and Table 2 show that the fitting equations of the first part (50–200 s, before peak counts) of 7–10  $\mu\text{m}$  and 10–15  $\mu\text{m}$  floc formation and transformation curves with dosages coagulation, respectively.

**Table 1.** Fitting equation of 7–10  $\mu\text{m}$  floc formation and transformation with dosages coagulation

Dosing	Fitting equation	Correlation coefficient (R)
Al 0.3 $\text{mg L}^{-1}$	$c = 1109.04 + 0.54 t$	0.917
Al 0.6 $\text{mg L}^{-1}$	$c = 1054.45 + 2.90 t$	0.982
Al 0.8 $\text{mg L}^{-1}$	$c = 978.51 + 6.12 t$	0.991
Al 1.0 $\text{mg L}^{-1}$	$c = 983.06 + 6.61 t$	0.993
Al 1.2 $\text{mg L}^{-1}$	$c = 1042.33 + 9.83 t$	0.999
Al 1.6 $\text{mg L}^{-1}$	$c = 1417.61 + 8.80 t$	0.990
Al 2.0 $\text{mg L}^{-1}$	$c = 1559.70 + 8.16 t$	0.984
Al 2.3 $\text{mg L}^{-1}$	$c = 1870.66 + 6.84 t$	0.993
Al 2.5 $\text{mg L}^{-1}$	$c = 1824.88 + 7.91 t$	0.944
Al 3.0 $\text{mg L}^{-1}$	$c = 2244.86 + 6.42 t$	0.995

**Table 2.** Fitting equation of 10–15  $\mu\text{m}$  floc formation and transformation with dosages coagulation

Dosing	Fitting equation	Correlation coefficient (R)
Al 0.3 mg $\text{L}^{-1}$	$c = 203.79 + 0.018 t$	0.269
Al 0.6 mg $\text{L}^{-1}$	$c = 176.03 + 0.50 t$	0.950
Al 0.8 mg $\text{L}^{-1}$	$c = 153.16 + 1.15 t$	0.981
Al 1.0 mg $\text{L}^{-1}$	$c = 174.32 + 1.24 t$	0.980
Al 1.2 mg $\text{L}^{-1}$	$c = 95.05 + 2.73 t$	0.985
Al 1.6 mg $\text{L}^{-1}$	$c = 102.69 + 3.48 t$	0.993
Al 2.0 mg $\text{L}^{-1}$	$c = 102.56 + 3.60 t$	0.999
Al 2.3 mg $\text{L}^{-1}$	$c = 260.61 + 2.77 t$	0.977
Al 2.5 mg $\text{L}^{-1}$	$c = 217.38 + 3.35 t$	0.896
Al 3.0 mg $\text{L}^{-1}$	$c = 284.66 + 3.45 t$	0.992

The two tables show that the most fitting equations of the particle counts curves are quite well fitted with linear equation. Nearly all of the correlation coefficients (R) are above 0.90. In Table 1 (7–10  $\mu\text{m}$ ) the correlation coefficients are from 0.982 to 0.990 as Al from 0.6–1.6 mg  $\text{L}^{-1}$ ; in Table 2 (10–15  $\mu\text{m}$ ) the correlation coefficients are from 0.950 to 0.999 as Al from 0.6–2.0 mg  $\text{L}^{-1}$ . This means that in smaller flocs (7–10  $\mu\text{m}$ ) growth curves the fitting equation are quite fitted linear equations at various dosage range (Al: 0.6–1.6 mg  $\text{L}^{-1}$ ); while the fitting equations are quite fitted with linear equations at various dosage range (0.6–2.0 mg  $\text{L}^{-1}$ ) in 10–15  $\mu\text{m}$  flocs growth curves.

The two tables also show that the slopes of the fitting equations of the flocs are larger for the smaller flocs growth curves (Table 1, 7–10  $\mu\text{m}$ ) than for floc growth curves in Table 2 (10–15  $\mu\text{m}$ ). In Table 1 the slopes are from 2.90–8.16 compared with those of 0.50–3.60 in Table 2 (10–15  $\mu\text{m}$ ) at the same dosages (Al: 0.6–2.0 mg  $\text{L}^{-1}$ ). This demonstrates that the smaller flocs grow faster and then the larger flocs.

Table 1 and Table 2 indicate that the floc growth curves could be used for monitoring the flocs growth correlated to the dosage and sedimentation results (Fig. 3). Especially, the slopes of the floc growth curves are very important. It could be seen that the sharper slope of the floc growth curves the better the sedimentation results, and for a dosage range between 2 and 3 mg  $\text{L}^{-1}$  is located in the best sedimentation result range. So in practice it should be possible to monitor the floc growth curves and analyze the coefficients of various flocs growth curves with dosages and use the results to control the dosing of coagulant or flocculants and estimate the efficiencies of the coagulation and flocculation.

The laser particle counter used as a monitor to detect the coagulation and flocculation has many advantages. It is able to record counts in 6 separate size channels, and the ranges are 2–3  $\mu\text{m}$ , 3–5  $\mu\text{m}$ , 5–7  $\mu\text{m}$ , 7–10  $\mu\text{m}$ ,

10–15  $\mu\text{m}$  and  $>15 \mu\text{m}$ , respectively and it covers the main range of the floc growth in the coagulation and the flocculation process. So the result can supply more correct and precise description than many flocculation detection methods especially in floc distribution description. This could supply much valuable data in the analysis of coagulation, flocculation, and sedimentation, and even in the following filtration process. Also the response time from the sampling to the monitor in the test is only 45 s; it shows that the delay time is very short and could respond very quickly.

## CONCLUSION

The experiments show that the floc formation and floc size distribution can be well monitored by online laser particle counter. Also the optimum dosage has a good relationship with the velocity of floc formation and floc size transformation. The results show that it is feasible to use particle counter as a detector and perhaps as a method of dosage control. However, there are several aspects that need further investigation.

## REFERENCES

1. Jarvis, P., Jefferson, B., Gregory, J., and Parsons, S.A. (2005) A review of floc strength and breakage. *Water Res.*, 39: 3121–3137.
2. Dentel, S.K. and Kingery, K.M. (1989) Using streaming current detectors in water treatment. *J. Am. Water Works Assoc.*, 81 (3): 85–94.
3. Gregory, J. and Dupont, V. (2001) Properties of flocs produced by water treatment coagulants. *Water Sci. Technol.*, 44: 231–236.
4. Yukselen, M.A. and Gregory, J. (2004) The reversibility of floc breakage. *Int. J. Miner. Process.*, 73: 251–259.
5. Gregory, J. and Nelson, D.W. (1986) Monitoring of aggregates flowing suspension. *Colloids Surf.*, 18: 175–188.
6. McCurdy, K., Carlson, K., and Gregory, D. (2004) Floc morphology and cyclic shearing recovery: comparison of alum and polyaluminium chloride coagulants. *Water Res.*, 38: 486–494.
7. Leentvaar, J. and Rebhun, M. (1983) Strength of ferric hydroxide flocs. *Water Res.*, 17: 895–902.
8. Ducoste, J.J. and Clark, M.M. (1998) The influence of tank size and impeller geometry on turbulent flocculation: I. *Experimental. Environ. Eng. Sci.*, 15 (3): 215–224.
9. Chakraborti, R.K., Atkinson, J.F., and Van Benschoten, J.E. (2000) Characterisation of alum floc by image processing. *Environ. Sci. Technol.*, 34 (18): 3969–3979.
10. Bache, D.H. and Rasool, E.R. (2001) Characteristics of aluminohumic flocs in relation to DAF performance. *Water Sci. Technol.*, 43 (8): 203–208.
11. Wang, X.C., Jin, P.K., and Gregory, J. (2002) Structure of Al-humic flocs and their removal at slightly acidic and neutral pH. *Water Sci. Technol.: Water Supply*, 2 (2): 99–106.

12. Spicer, P.T., Pratsinis, S.E., Raper, J., Amal, R., Bushell, G., and Meesters, G. (1998) Effect of shear schedule on particle size, density, and structure during flocculation in stirred tanks. *Powder Technology*, 97 (1): 26–34.
13. Biggs, C.A. and Lant, P.A. (2000) Activated sludge flocculation: on-line determination of floc size and the effect of shear. *Water Res.*, 34: 2542–2550.
14. Farrow, J. and Warren, L. (1993) Measurement of the size of aggregates in suspension. In *Coagulation and Flocculation—Theory and Applications*, Dobias, B. (ed.); Marcel Dekker Inc.: New York, USA, 391–426.
15. Mejia, A.C. and Cisneros, B.J. (2000) Particle size distribution (PSD) obtained in effluents from an advanced primary treatment process using different coagulants. In *Chemical Water and Wastewater Treatment VI*. Hahn, H., Hoffmann, E., and Odegaard, H. (eds.); Springer: Berlin, 257–268.